

Positioning Error Probabilities for Some Forms of Center-of-Gravity Algorithm Calculated with the Cumulative Distributions. Part II

Gregorio Landi^{a*}, Giovanni E. Landi^b

^a Dipartimento di Fisica e Astronomia, Università di Firenze and INFN
Largo E. Fermi 2 (Arcetri) 50125, Firenze, Italy

^b ArchonVR S.a.g.l.,
Via Cisieri 3, 6900 Lugano, Switzerland.

February 25, 2021

Abstract

To complete a previous work, the probability density functions for the errors in the center-of-gravity as positioning algorithm are derived with the usual methods of the cumulative distribution functions. These methods introduce substantial complications compared to the approaches used in a previous publication on similar problems. The combinations of random variables considered are: $X_{g3} = \theta(x_2 - x_1)(x_1 - x_3)/(x_1 + x_2 + x_3) + \theta(x_1 - x_2)(x_1 + 2x_4)/(x_1 + x_2 + x_4)$ and $X_{g4} = (\theta(x_4 - x_5)(2x_4 + x_1 - x_3)/(x_1 + x_2 + x_3 + x_4) + \theta(x_5 - x_4)(x_1 - x_3 - 2x_5)/(x_1 + x_2 + x_3 + x_5))$. The complete and partial forms of the probability density functions of these expressions of the center-of-gravity algorithms are calculated for general probability density functions of the observation noise. The cumulative probability distributions are the essential steps in this study, never calculated elsewhere.

Contents

1	Introduction	2
2	The discontinuity around $x \approx 1/2$ of the three strip COG (COG₃)	2
2.1	Sign conventions	3
2.2	A better reference system	5
2.3	Integrals for $x > 1/2$	7
2.4	COG ₃ probability density function	9
3	Probability distributions for the four strip COG (COG₄)	10
3.1	COG ₄ probability distributions with only right strip or left strip	10
3.2	Complete probability distribution for $P_{xg4}(x)$	14
4	Summary and conclusions	15

*Corresponding author. Gregorio.Landi@fi.infn.it

1 Introduction

Specialized probability density functions (PDFs) are essential instruments for track fitting in heteroscedastic systems, that must be constructed for the positioning algorithms of the track observations (hits). The demonstrations of refs [1, 2] require the appropriate variances for each hit of the detector to obtain optimal fits. The variance calculations and the search of the maximum likelihood are essentially based on these PDFs, and, being non-Gaussian, the results of the maximum likelihood add further improvements to the track resolution beyond the least-squares method. In fact, the PDFs of the most frequently used positioning algorithms turn out very different from Gaussian PDFs, with Cauchy-Agnesi-like tails due to the non-linearity of the algorithms. In principle, the PDFs have infinite variances that is improperly handled by methods based on variance minimizations, hence, drastic modification must be introduced to extract finite variances. References [3, 4] was devoted to obtain the error PDFs for some forms of the center of gravity (COG) positioning algorithms with a the simplified method of ref. [5]. That method obtains a PDF without using the cumulative distribution, essential instead in the standard method [6]. To complete that result, this paper is devoted to compute the PDFs of the COG algorithms of ref. [4] with the use of the cumulative distribution, as we did in ref. [7] for the PDFs the COG algorithms of ref. [3]. The calculation of the cumulative distribution is very long and complicated, requiring many integrations on sectors of the space of the random variables given by the noisy strip signals. However, this approach was the first one we used to compute the PDFs extensively utilized in ref. [8] and in all the searches of likelihood maximums. The following sections are our summary notes of those developments. We can not hide the complexity of the likelihood method and the extraction of the individual hit error PDFs to insert in the likelihood. The gain in resolution observed in the simulations of refs. [5, 8, 9] largely justifies these increases of complexity. In addition to this, the demonstrations of refs. [1, 2] show the non-optimality of the use of the standard least squares method (optimum only for homoscedastic systems) obliging to utilize more elaborated procedures.

To illustrate the power of these procedures, we introduced in ref. [9] a very simple toy model to clearly show the drastic gains in the parameter resolution compared to the standard least squares. The toy model requires few lines of MATLAB-code [10] to be implemented and could be an easy teste of heteroscedasticity. In fact, that toy model was extensively explored in ref. [11] well outside the range of our parameters with very interesting results. Instead, ref. [12] sustains that the results of the toy model are interesting only for a small number of observations. Going to large numbers one obtains results *compatible with common wisdom. Neither homoscedasticity nor heteroscedasticity are found to play any role in the matter.* This statement of [12] is really surprising, given that, inserting its plots of the two fit types in the same figure, the direct comparison clearly shows large differences in rate of growth and amplitude. All in favor of heteroscedasticity, albeit with a rate of growth not as rapid as that for the observation numbers of ref. [9]. Evidently, the addition of a good observation around to hundred of them has a much less effect than around to ten. However, those large numbers have no physical meaning for our aim of particle tracking.

To handle properly the intrinsic heteroscedasticity of a tracker system, the following PDFs are only first steps. Other tools are essential and require further details, shortly outlined in ref. [5, 8]. For evident reason, all these required developments are split in parts and published separately.

2 The discontinuity around $x \approx 1/2$ of the three strip COG (COG₃)

Reference [7] (and ref. [3]) account for the COG₃ in its simplest form, without the introduction of the effects of the noise in promoting a lateral strip to become the seed strip (that with the maximum signal). This noise effect produces gaps/discontinuities in the PDF of the COG₃ algorithm, gaps/discontinuities essential for a consistent likelihood. The COG₃ histograms show, for large signal distributions, reductions of the data density around $\pm 1/2$ as discussed in ref. [4] and with more details in refs. [13, 14].

The PDFs of the COG₃ around the discontinuity of $x_{g3} \approx 1/2$ will be calculated with the standard method [6]. As first step we have to obtain the cumulative distribution, its differentiation gives the PDF. In this case, the combined probability of four strips has to be considered. The three strips of the COG₃ in the range $-1/2 \ll x_{g3} \ll 1/2$ and the fourth strip when the $x_{g3} \approx 1/2$ and the noise is can move the strip with the maximum signal to the strip to its right. Or to its left for $x_{g3} \approx -1/2$.

To save the conventions of the previous approaches we will indicate the strips of our interest (from left to right) $\langle 3 \rangle, \langle 2 \rangle, \langle 1 \rangle, \langle 4 \rangle$. The gap/discontinuity is present when the maximum-strip signal moves from the strip $\langle 2 \rangle$ to the strip $\langle 1 \rangle$ and the COG₃, formerly calculated with signals of the strips $\langle 3 \rangle, \langle 2 \rangle, \langle 1 \rangle$, must be calculated with signals of $\langle 2 \rangle, \langle 1 \rangle, \langle 4 \rangle$.

2.1 Sign conventions

The position of the strips are defined relatively to the strip with the maximum signal, negative positions to the left, positive positions to the right. When the strip with maximum signal is $\langle 2 \rangle$ and $\{x_i, i = 1, 2, \dots\}$ are the signals of the strips, the COG₃ expression x_{g3} is:

$$x_{g3} = \frac{x_1 - x_3}{x_1 + x_2 + x_3} \quad (1)$$

When x_1 is the maximum strip signal, x_{g3} is given by:

$$x_{g3} = \frac{x_4 - x_2}{x_1 + x_2 + x_4} \quad (2)$$

This convention is impractical for our needs because when $x_2 \approx x_1 \gg x_3, x_4$ the previous definition generates a transition of x_{g3} from $1/2$ to $-1/2$. It is fundamental to use in any case the center of the strip $\langle 2 \rangle$ as origin of the COG reference system. Now eq. 2 becomes:

$$x_{g3} = \frac{x_4 - x_2}{x_1 + x_2 + x_4} + 1 = \frac{x_1 + 2x_4}{x_1 + x_2 + x_4} \quad (3)$$

and the transition of the leading strip increases the values of x_{g3} beyond $1/2$. The (almost always) positive value of x_3 or x_4 impedes to x_{g3} to be equal to $1/2$. Negative values of the strip signals allow $x_{g3} = 1/2$, evidently the negative values of x_i are produced by the noise for very low signals.

The PDF of x_{g3} will be obtained differentiating the cumulative probability to have the x_{g3} values less than a given value. The following naming convention will be used in place of the $\{x_i\}$:

$$x_1 = \xi, \quad x_2 = \eta, \quad x_3 = \beta \quad x_4 = \gamma$$

giving

$$x_{g3} = \frac{\xi - \beta}{\xi + \eta + \beta} \quad x_{g3} \leq 0.5$$

$$x_{g3} = \frac{2\gamma + \xi}{\gamma + \eta + \xi} \quad x_{g3} > 0.5.$$

In ref. [7], we explored the conditions imposed by x_{g3} to be lower than a given value x :

$$\frac{\xi - \beta}{\xi + \eta + \beta} < x, \quad (4)$$

with its two possibilities $\xi + \eta + \beta > 0$ and $\xi + \eta + \beta < 0$. In any case we have two limiting planes:

$$\xi(1-x) + \beta(-1-x) - \eta x = 0 \quad \text{and} \quad \xi + \eta + \beta = 0.$$

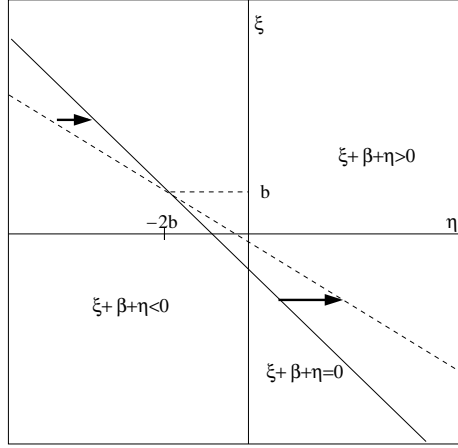


Figure 1: Sector of the plane (η, ξ) where $\xi + \eta + \beta > 0$ or $\xi + \eta + \beta < 0$ and the boundary $\xi + \eta + \beta = 0$, the dashed line is the line $\xi(1-x) + b(-1-x) - \eta x = 0$ for negative x , the arrows indicate the η integration-paths for $(\xi + \eta + \beta) < 0$ and for $(\xi + \eta + \beta) > 0$

Let us see the case with $\beta > 0$ and $\beta = b$. The traces of the two planes are these of fig. 1. The intersection point is $\{-2b, b\}$ and it changes with β . Now we have to consider a change of algorithm when $\xi > \eta$ (with the signals this implies $x_1 > x_2$). The plane ξ, η must be separated in two parts along the line $\xi = \eta$ below this line we have the algorithm with the random variables β, ξ, η with part of the lines of fig. 1. Above this line we have the algorithm with the random variables γ, ξ, η Let us explore the integration regions for $x < 0$ and $\beta \neq 0$. Figures 2 and 3 illustrate the conditions with $\beta \geq 0$ (left side) and $\beta < 0$ (right side) and similarly for the variable γ .

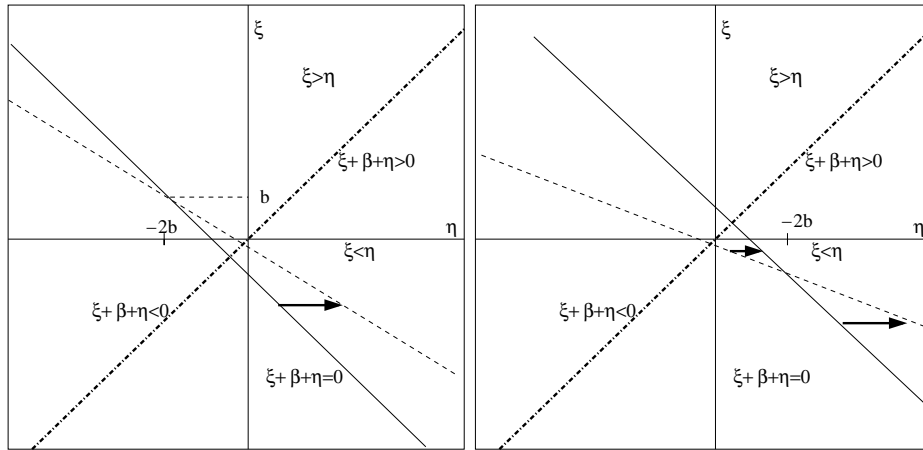


Figure 2: Sector of the plane (η, ξ) where $\xi + \eta + \beta > 0$ or $\xi + \eta + \beta < 0$ and its boundary $\xi + \eta + \beta = 0$, the dashed line is the line $\xi(1-x) + b(-1-x) - \eta x = 0$ for negative x . The arrows indicate the η integration-paths for $(\xi + \eta + \beta) < 0$ and for $(\xi + \eta + \beta) > 0$. One boundary of the integration regions is the line $\xi = \eta$

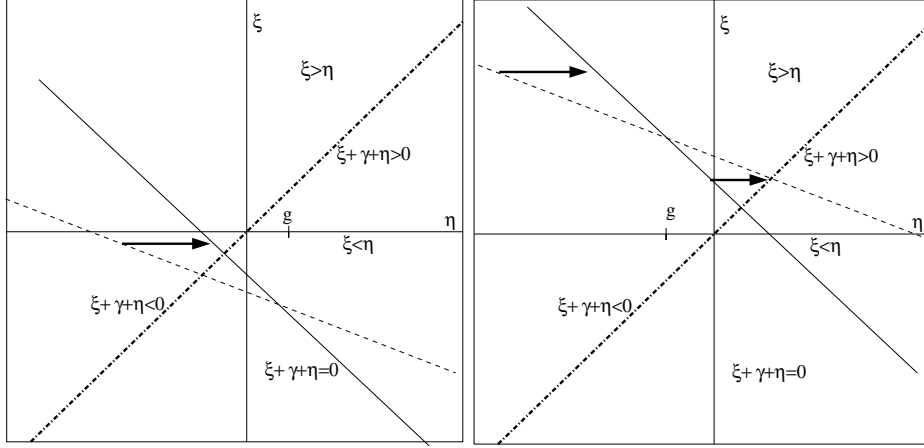


Figure 3: Sector of the plane (η, ξ) where $\xi + \eta + \gamma > 0$ or $\xi + \eta + \gamma < 0$ and its boundary $\xi + \eta + \gamma = 0$, the dashed line is the line with $\gamma = g$ and $\xi(1-x) + g(2-x) - \eta x = 0$ for negative x . The arrows indicate the η integration-paths for $(\xi + \eta + \gamma) < 0$ and for $(\xi + \eta + \gamma) > 0$, one boundary of the integration regions is the dash-dotted line $\xi = \eta$

2.2 A better reference system

Observing the figures 1, 2 and 3, we see that the reference system based on the two orthogonal lines $\xi + \eta + \beta = 0$ and $\xi = \eta$ has some special property. For any x , the integration regions have a boundary on the line $\xi + \eta + \beta = 0$, and the variation of x implies a rotation of the dashed line around a fixed point (for fixed $\beta = b$). For $x \geq 1/2$ a part of the plane ξ, η is fully covered and the integration regions change drastically. With this reference system we have to distinguish two range of x -values: $x \leq 1/2$ and $x > 1/2$, this is in fact the point in which we have a discontinuity.

Let us write the form of the new variables (with β):

$$\begin{aligned} \eta' &= \frac{\eta - \xi}{\sqrt{2}} & \eta &= \frac{\xi' + \eta'}{\sqrt{2}} - \frac{\beta}{2} \\ \xi' &= \frac{\eta + \xi + \beta}{\sqrt{2}} & \xi &= \frac{\xi' - \eta'}{\sqrt{2}} - \frac{\beta}{2} \end{aligned} \quad (5)$$

and similarly for the side with γ :

$$\begin{aligned} \eta' &= \frac{\eta - \xi}{\sqrt{2}} & \eta &= \frac{\xi' + \eta'}{\sqrt{2}} - \frac{\gamma}{2} \\ \xi' &= \frac{\eta + \xi + \gamma}{\sqrt{2}} & \xi &= \frac{\xi' - \eta'}{\sqrt{2}} - \frac{\gamma}{2} \end{aligned} \quad (6)$$

The following integrals are those in the regions of figure 4 for $\beta \geq 0$ and $\beta < 0$.

$$\begin{aligned} F_1^{xg^3}(x) &= \\ & \int_0^{+\infty} d\beta P_3(\beta) \int_0^{+\infty} d\eta' \int_0^{\frac{\sqrt{2}\eta'+3\beta}{\sqrt{2}(1-2x)}} d\xi' P_2\left(\frac{\xi' + \eta'}{\sqrt{2}} - \frac{\beta}{2}\right) P_1\left(\frac{\xi' - \eta'}{\sqrt{2}} - \frac{\beta}{2}\right) + \\ & \int_{-\infty}^0 d\beta P_3(\beta) \int_0^{-\frac{3\beta}{\sqrt{2}}} d\eta' \int_0^{\frac{\sqrt{2}\eta'+3\beta}{\sqrt{2}(1-2x)}} d\xi' P_2\left(\frac{\xi' + \eta'}{\sqrt{2}} - \frac{\beta}{2}\right) P_1\left(\frac{\xi' - \eta'}{\sqrt{2}} - \frac{\beta}{2}\right) + \\ & \int_{-\infty}^0 d\beta P_3(\beta) \int_{-\frac{3\beta}{\sqrt{2}}}^{+\infty} d\eta' \int_0^{\frac{\sqrt{2}\eta'+3\beta}{\sqrt{2}(1-2x)}} d\xi' P_2\left(\frac{\xi' + \eta'}{\sqrt{2}} - \frac{\beta}{2}\right) P_1\left(\frac{\xi' - \eta'}{\sqrt{2}} - \frac{\beta}{2}\right) \end{aligned} \quad (7)$$

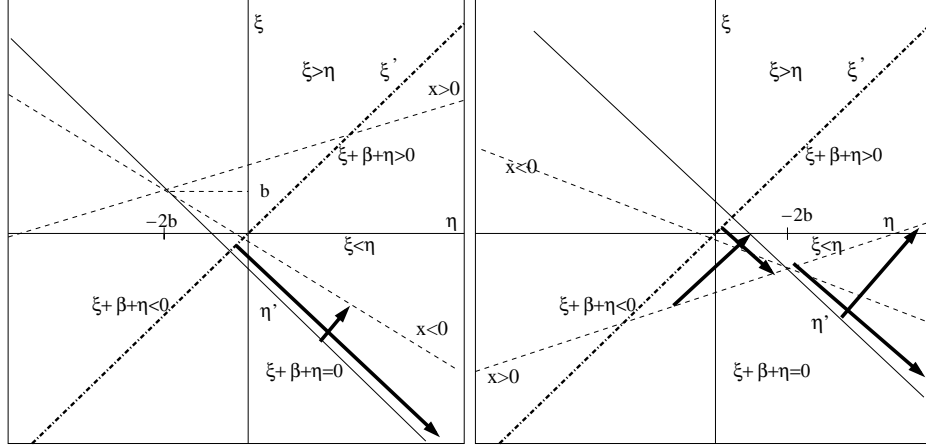


Figure 4: The left figure is the case with $\beta > 0$, the right side is for $\beta < 0$. The dashed lines are the line $\xi(1-x) + b(-1-x) - \eta x = 0$ for $x > 0$ and $x < 0$, the continuous line is the new axis η' and the dash-dotted line is the new axis ξ' . For $x < 1/2$, the arrows indicate the η' and ξ' integration-paths for $(\xi + \eta + \beta) < 0$ and for $(\xi + \eta + \beta) > 0$

The integrals to the regions with $\eta' < 0$ (figure 5) depend from the variable γ and they are:

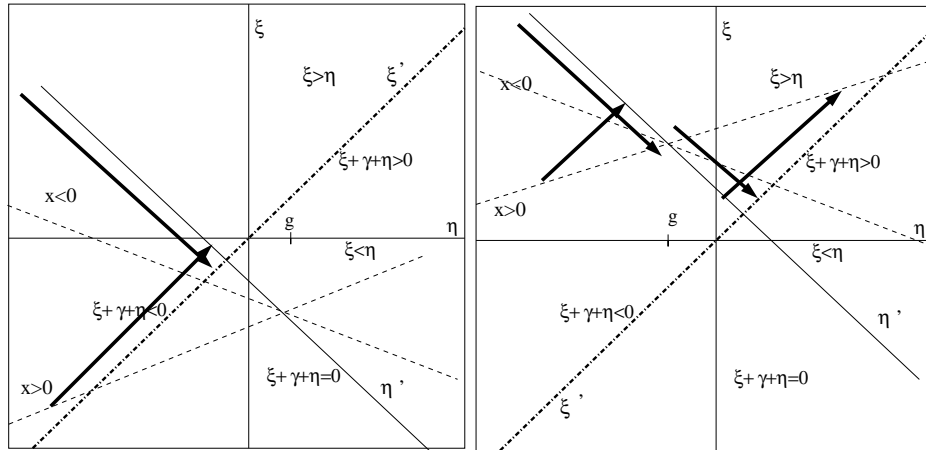


Figure 5: Sector of the plane (η, ξ) where $\xi + \eta + \gamma > 0$ or $\xi + \eta + \gamma < 0$ and its boundary $\xi + \eta + \gamma = 0$, the dashed line is the line with $\gamma = g$ and $\xi(1-x) + g(2-x) - \eta x = 0$. For negative x , the arrows indicate the η integration-paths for $(\xi + \eta + \gamma) < 0$ and for $(\xi + \eta + \gamma) > 0$ one of the boundary of the integration regions is the dash-dotted line $\xi = \eta$

$$\begin{aligned}
F_2^{xg3}(x) = & \int_0^{+\infty} d\gamma P_4(\gamma) \int_{-\infty}^0 d\eta' \int_0^{\frac{\sqrt{2}\eta' - 3\gamma}{\sqrt{2}(1-2x)}} d\xi' P_2\left(\frac{\xi' + \eta'}{\sqrt{2}} - \frac{\gamma}{2}\right) P_1\left(\frac{\xi' - \eta'}{\sqrt{2}} - \frac{\gamma}{2}\right) + \\
& \int_{-\infty}^0 d\gamma P_4(\gamma) \int_{\frac{3\gamma}{\sqrt{2}}}^0 d\eta' \int_0^{\frac{\sqrt{2}\eta' - 3\gamma}{\sqrt{2}(1-2x)}} d\xi' P_2\left(\frac{\xi' + \eta'}{\sqrt{2}} - \frac{\gamma}{2}\right) P_1\left(\frac{\xi' - \eta'}{\sqrt{2}} - \frac{\gamma}{2}\right) + \\
& \int_{-\infty}^0 d\gamma P_4(\gamma) \int_{-\infty}^{\frac{3\gamma}{\sqrt{2}}} d\eta' \int_0^{\frac{\sqrt{2}\eta' - 3\gamma}{\sqrt{2}(1-2x)}} d\xi' P_2\left(\frac{\xi' + \eta'}{\sqrt{2}} - \frac{\gamma}{2}\right) P_1\left(\frac{\xi' - \eta'}{\sqrt{2}} - \frac{\gamma}{2}\right)
\end{aligned} \tag{8}$$

It is easy to verify that in the limit of $x \rightarrow -\infty$ all the integrals in ξ' converge to zero and the cumulative function is zero, as it must be. Geometrically, this means that the integration region below the dashed lines of figures 4 and 5 disappear due to its coincidence with the ξ' axis.

2.3 Integrals for $x > 1/2$

Let us see the forms of the integrals for $x > 1/2$, here some integrals are extended to fixed regions of the plane $\{\xi', \eta'\}$. The following figures 6 and 7 illustrate the integration regions for $x > 1/2$. The regions, that are unaffected by the x variations, contribute to the cumulative distribution function, but are irrelevant for the extraction of the probability distribution. We will use them for a consistency check of the cumulative distribution function with x going to infinite.

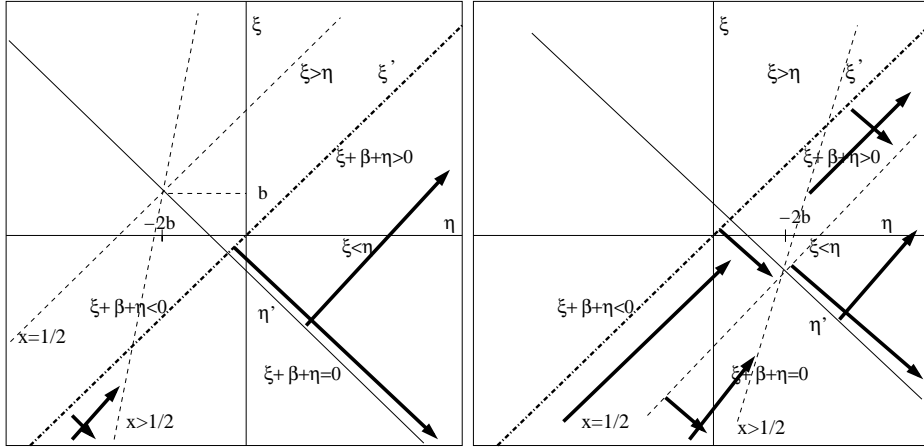


Figure 6: The left figure is the case with $\beta > 0$, the right side is for $\beta < 0$. The dashed lines are the line $\xi(1-x) + b(-1-x) - \eta x = 0$ for $x > 0$ and $x < 0$, the continuous line is the new axis η' and the dash-dotted line is the new axis ξ' . For $x < 1/2$, the arrows indicate the η' and ξ' integration-paths for $(\xi + \eta + \beta) < 0$ and for $(\xi + \eta + \beta) > 0$

Let us calculate the forms of the integrals for the random variable β . In this case $\eta > \xi$ and we are always below the line $\xi = \eta$ or for positive values of η' .

$$\begin{aligned}
F_3^{xg^3}(x) = & \int_0^{+\infty} d\beta P_3(\beta) \int_0^{+\infty} d\eta' \int_0^{+\infty} d\xi' P_2\left(\frac{\xi' + \eta'}{\sqrt{2}} - \frac{\beta}{2}\right) P_1\left(\frac{\xi' - \eta'}{\sqrt{2}} - \frac{\beta}{2}\right) + \\
& \int_0^{+\infty} d\beta P_3(\beta) \int_0^{+\infty} d\eta' \int_{-\infty}^{\frac{\sqrt{2}\eta' + 3\beta}{\sqrt{2}(1-2x)}} d\xi' P_2\left(\frac{\xi' + \eta'}{\sqrt{2}} - \frac{\beta}{2}\right) P_1\left(\frac{\xi' - \eta'}{\sqrt{2}} - \frac{\beta}{2}\right) + \\
& \int_{-\infty}^0 d\beta P_3(\beta) \int_0^{-\frac{3\beta}{\sqrt{2}}} d\eta' \int_{-\infty}^0 d\xi' P_2\left(\frac{\xi' + \eta'}{\sqrt{2}} - \frac{\beta}{2}\right) P_1\left(\frac{\xi' - \eta'}{\sqrt{2}} - \frac{\beta}{2}\right) + \\
& \int_{-\infty}^0 d\beta P_3(\beta) \int_{-\frac{3\beta}{\sqrt{2}}}^{+\infty} d\eta' \int_{-\infty}^{\frac{\sqrt{2}\eta' + 3\beta}{\sqrt{2}(1-2x)}} d\xi' P_2\left(\frac{\xi' + \eta'}{\sqrt{2}} - \frac{\beta}{2}\right) P_1\left(\frac{\xi' - \eta'}{\sqrt{2}} - \frac{\beta}{2}\right) + \\
& \int_{-\infty}^0 d\beta P_3(\beta) \int_0^{-\frac{3\beta}{\sqrt{2}}} d\eta' \int_{-\infty}^{+\infty} d\xi' P_2\left(\frac{\xi' + \eta'}{\sqrt{2}} - \frac{\beta}{2}\right) P_1\left(\frac{\xi' - \eta'}{\sqrt{2}} - \frac{\beta}{2}\right) + \\
& \int_{-\infty}^0 d\beta P_3(\beta) \int_{-\frac{3\beta}{\sqrt{2}}}^{+\infty} d\eta' \int_0^{+\infty} d\xi' P_2\left(\frac{\xi' + \eta'}{\sqrt{2}} - \frac{\beta}{2}\right) P_1\left(\frac{\xi' - \eta'}{\sqrt{2}} - \frac{\beta}{2}\right)
\end{aligned} \tag{9}$$

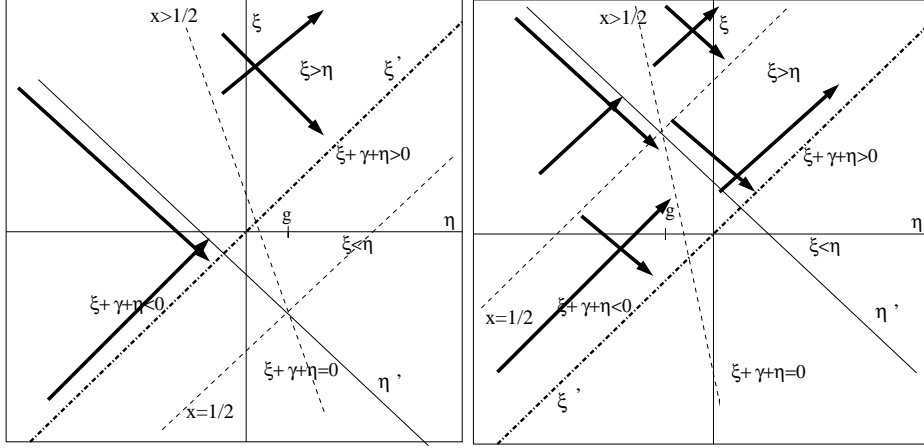


Figure 7: Sector of the plane (η, ξ) where $\xi + \eta + \gamma > 0$ or $\xi + \eta + \gamma < 0$ and its boundary $\xi + \eta + \gamma = 0$, the dashed line is the line with $\gamma = g \xi (1 - x) + g(2 - x) - \eta x = 0$ for negative x , the arrows indicate the η integration-paths for $(\xi + \eta + \gamma) < 0$ and for $(\xi + \eta + \gamma) > 0$ one of the boundary of the integration regions is the dash-dotted line $\xi = \eta$

The integrals with the random variable $\xi > \eta$ are the following:

$$\begin{aligned}
F_4^{xg^3}(x) = & \int_0^{+\infty} d\gamma P_4(\gamma) \int_{-\infty}^0 d\eta' \int_{-\infty}^0 d\xi' P_2\left(\frac{\xi' + \eta'}{\sqrt{2}} - \frac{\gamma}{2}\right) P_1\left(\frac{\xi' - \eta'}{\sqrt{2}} - \frac{\gamma}{2}\right) + \\
& \int_0^{+\infty} d\gamma P_4(\gamma) \int_{-\infty}^0 d\eta' \int_{\frac{\sqrt{2}\eta' - 3\gamma}{\sqrt{2}(1-2x)}}^{+\infty} d\xi' P_2\left(\frac{\xi' + \eta'}{\sqrt{2}} - \frac{\gamma}{2}\right) P_1\left(\frac{\xi' - \eta'}{\sqrt{2}} - \frac{\gamma}{2}\right) + \\
& \int_{-\infty}^0 d\gamma P_4(\gamma) \int_{-\infty}^{\frac{3\gamma}{\sqrt{2}}} d\eta' \int_{-\infty}^0 d\xi' P_2\left(\frac{\xi' + \eta'}{\sqrt{2}} - \frac{\gamma}{2}\right) P_1\left(\frac{\xi' - \eta'}{\sqrt{2}} - \frac{\gamma}{2}\right) + \\
& \int_{-\infty}^0 d\gamma P_4(\gamma) \int_{\frac{3\gamma}{\sqrt{2}}}^0 d\eta' \int_{-\infty}^{\frac{\sqrt{2}\eta' - 3\gamma}{\sqrt{2}(1-2x)}} d\xi' P_2\left(\frac{\xi' + \eta'}{\sqrt{2}} - \frac{\gamma}{2}\right) P_1\left(\frac{\xi' - \eta'}{\sqrt{2}} - \frac{\gamma}{2}\right) \\
& \int_{-\infty}^0 d\gamma P_4(\gamma) \int_{-\infty}^{\frac{3\gamma}{\sqrt{2}}} d\eta' \int_{\frac{\sqrt{2}\eta' - 3\gamma}{\sqrt{2}(1-2x)}}^{+\infty} d\xi' P_2\left(\frac{\xi' + \eta'}{\sqrt{2}} - \frac{\gamma}{2}\right) P_1\left(\frac{\xi' - \eta'}{\sqrt{2}} - \frac{\gamma}{2}\right) + \\
& \int_{-\infty}^0 d\gamma P_4(\gamma) \int_{\frac{3\gamma}{\sqrt{2}}}^0 d\eta' \int_0^{+\infty} d\xi' P_2\left(\frac{\xi' + \eta'}{\sqrt{2}} - \frac{\gamma}{2}\right) P_1\left(\frac{\xi' - \eta'}{\sqrt{2}} - \frac{\gamma}{2}\right)
\end{aligned} \tag{10}$$

To verify the consistency of the cumulative probability we must have:

$$\lim_{x \rightarrow +\infty} F^{xg^3}(x) = \lim_{x \rightarrow +\infty} (F_3^{xg^3}(x) + F_4^{xg^3}(x)) = 1 \tag{11}$$

For $x \rightarrow +\infty$ the limit of the integrals that are expressed by $(\sqrt{2}\eta' - 3\gamma)/(\sqrt{2}(1 - 2x))$ becomes zero and the first two of F_4 can be added giving an integration on ξ' from $-\infty$ to $+\infty$. The third and the fourth produce an integral on η' from $-\infty$ to zero and an integral on ξ' from $-\infty$ and 0. It is easy to see the result (the integrations on the probability function of the random variable γ and β , present respectively in the first and second integral, are omitted due to their trivial values equal to one):

$$\begin{aligned}
\lim_{x \rightarrow +\infty} F_3^{xg^3}(x) &= \int_0^{+\infty} d\eta' \int_{-\infty}^{+\infty} d\beta P_3(\beta) \int_{-\infty}^{+\infty} d\xi' P_2\left(\frac{\xi' + \eta'}{\sqrt{2}} - \frac{\beta}{2}\right) P_1\left(\frac{\xi' - \eta'}{\sqrt{2}} - \frac{\beta}{2}\right) \\
\lim_{x \rightarrow +\infty} F_4^{xg^3}(x) &= \int_{-\infty}^0 d\eta' \int_{-\infty}^{+\infty} d\gamma P_4(\gamma) \int_{-\infty}^{+\infty} d\xi' P_2\left(\frac{\xi' + \eta'}{\sqrt{2}} - \frac{\gamma}{2}\right) P_1\left(\frac{\xi' - \eta'}{\sqrt{2}} - \frac{\gamma}{2}\right)
\end{aligned} \tag{12}$$

The observation of fig. 6 and fig. 7 for $x \rightarrow +\infty$ shows that the integration regions are independent from the parameters β and γ and the variable ξ' can be defined for $\beta = b = 0$ and $\gamma = g = 0$. Equation 12 becomes:

$$\begin{aligned}\lim_{x \rightarrow +\infty} F_3^{xg^3}(x) &= \int_0^{+\infty} d\eta' \int_{-\infty}^{+\infty} d\xi' P_2\left(\frac{\xi' + \eta'}{\sqrt{2}}\right) P_1\left(\frac{\xi' - \eta'}{\sqrt{2}}\right) \\ \lim_{x \rightarrow +\infty} F_4^{xg^3}(x) &= \int_{-\infty}^0 d\eta' \int_{-\infty}^{+\infty} d\xi' P_2\left(\frac{\xi' + \eta'}{\sqrt{2}}\right) P_1\left(\frac{\xi' - \eta'}{\sqrt{2}}\right)\end{aligned}\quad (13)$$

The integrals on β and γ are one for their normalization. The two remaining integrals sum together and all the space of the variables ξ and η is covered and their normalization gives eq. 11.

2.4 COG₃ probability density function

The differentiation of $F^{xg^3}(x)$ in x gives the probability density function $P_d^{xg^3}(x)$. The forms of $F^{xg^3}(x)$ for $x > 1/2$ and $x \leq 1/2$ give an identical expression upon differentiation.

$$\begin{aligned}P_d^{xg^3}(x) &= \frac{dF^{xg^3}(x)}{dx} = \\ &\int_0^{+\infty} d\beta P_3(\beta) \int_0^{+\infty} d\eta' P_2\left(\frac{\sqrt{2}(1-x)\eta' + \beta(1+x)}{1-2x}\right) P_1\left(\frac{\sqrt{2x}\eta' + \beta(1+x)}{1-2x}\right) \frac{2\eta' + 3\sqrt{2}\beta}{(1-2x)^2} \\ &+ \int_{-\infty}^0 d\beta P_3(\beta) \int_{-\frac{3\beta}{\sqrt{2}}}^{+\infty} d\eta' P_2\left(\frac{\sqrt{2}(1-x)\eta' + \beta(1+x)}{1-2x}\right) P_1\left(\frac{\sqrt{2x}\eta' + \beta(1+x)}{1-2x}\right) \frac{2\eta' + 3\sqrt{2}\beta}{(1-2x)^2} \\ &- \int_{-\infty}^0 d\beta P_3(\beta) \int_0^{-\frac{3\beta}{\sqrt{2}}} d\eta' P_2\left(\frac{\sqrt{2}(1-x)\eta' + \beta(1+x)}{1-2x}\right) P_1\left(\frac{\sqrt{2x}\eta' + \beta(1+x)}{1-2x}\right) \frac{2\eta' + 3\sqrt{2}\beta}{(1-2x)^2} \\ &- \int_0^{+\infty} d\gamma P_4(\gamma) \int_{-\infty}^0 d\eta' P_2\left(\frac{\sqrt{2}(1-x)\eta' - \gamma(2-x)}{1-2x}\right) P_1\left(\frac{\sqrt{2x}\eta' - \gamma(2-x)}{1-2x}\right) \frac{2\eta' - 3\sqrt{2}\gamma}{(1-2x)^2} \\ &+ \int_{-\infty}^0 d\gamma P_4(\gamma) \int_{\frac{3\gamma}{\sqrt{2}}}^0 d\eta' P_2\left(\frac{\sqrt{2}(1-x)\eta' - \gamma(2-x)}{1-2x}\right) P_1\left(\frac{\sqrt{2x}\eta' - \gamma(2-x)}{1-2x}\right) \frac{2\eta' - 3\sqrt{2}\gamma}{(1-2x)^2} \\ &+ \int_{-\infty}^0 d\gamma P_4(\gamma) \int_{-\infty}^{\frac{3\gamma}{\sqrt{2}}} d\eta' P_2\left(\frac{\sqrt{2}(1-x)\eta' - \gamma(2-x)}{1-2x}\right) P_1\left(\frac{\sqrt{2x}\eta' - \gamma(2-x)}{1-2x}\right) \frac{2\eta' - 3\sqrt{2}\gamma}{(1-2x)^2}\end{aligned}\quad (14)$$

Equation 14 can be recast in the form (explicitly positive):

$$\begin{aligned}P_d^{xg^3}(x) &= \frac{dF^{xg^3}(x)}{dx} = \\ &\int_{-\infty}^{+\infty} d\beta P_3(\beta) \int_0^{+\infty} d\eta' P_2\left(\frac{\sqrt{2}(1-x)\eta' + \beta(1+x)}{1-2x}\right) P_1\left(\frac{\sqrt{2x}\eta' + \beta(1+x)}{1-2x}\right) \frac{\text{abs}(2\eta' + 3\sqrt{2}\beta)}{(1-2x)^2} + \\ &\int_{-\infty}^{+\infty} d\gamma P_4(\gamma) \int_{-\infty}^0 d\eta' P_2\left(\frac{\sqrt{2}(1-x)\eta' - \gamma(2-x)}{1-2x}\right) P_1\left(\frac{\sqrt{2x}\eta' - \gamma(2-x)}{1-2x}\right) \frac{\text{abs}(2\eta' - 3\sqrt{2}\gamma)}{(1-2x)^2}\end{aligned}\quad (15)$$

Equation 15 is general for any x and any distribution of the four random variables. With a set of appropriate coordinate transformations the integrals of equation 2 of ref. [4] can be recast in this form. The denominators $(1-2x)^2$ allow to introduce a Dirac δ approximation around $x \approx 1/2$ as done in ref. [5] for the two strip COG around $x \approx 0$. The Cauchy-Agnesi tails are evident in 15. Renaming the random variables and the due change of x , eq. 15 can be used around the gap/discontinuity $x \approx -1/2$.

3 Probability distributions for the four strip COG (COG₄)

As discussed in ref. [13], the histograms of the COG algorithms with an even number of strips (and large signal distributions) have gaps/discontinuities around $x \approx 0$. Thus, as for the two strip COG, we have to separately study the addition of the right strip and the addition of the left strip.

3.1 COG₄ probability distributions with only right strip or left strip

Now we have to work in a four dimensional space. We will consider the two strips around the strip with the maximum signal and the forth strip to the right of these three. Let us recall our unusual strip ordering for the five strips required here (from left to right): $\langle 5 \rangle$, $\langle 3 \rangle$, $\langle 2 \rangle$, $\langle 1 \rangle$, $\langle 4 \rangle$. With the convention on the names of the strip signals:

$$x_5 = \psi, \quad x_3 = \beta, \quad x_2 = \eta, \quad x_1 = \xi, \quad x_4 = \gamma.$$

As always the maximum random variable is $x_2 = \eta$ and the center of the strip $\langle 2 \rangle$ is the origin of the axis for the COG₄ algorithm. In this reference system x_{g4} is:

$$x_{g4} = \frac{\xi - \beta + 2\gamma}{\xi + \eta + \beta + \gamma}$$

For $\beta = 0$, $\gamma = 0$ and $\xi + \eta > 0$ we have the plot of fig. 8 in general we have to explore the condition:

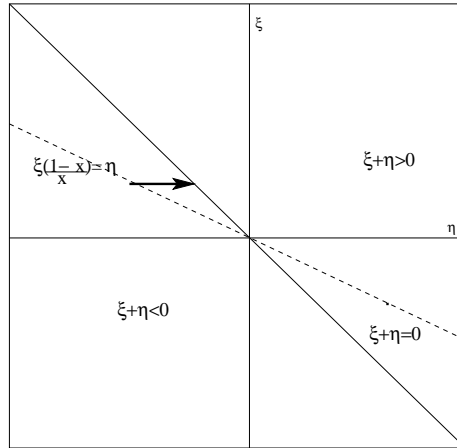


Figure 8: Sector of the plane (η, ξ) with $\beta = \gamma = 0$ where $\xi + \eta > 0$ or $\xi + \eta < 0$ and its boundary $\xi + \eta = 0$, the dashed line is the line $\xi(1-x)/x = \eta$ for negative x , the arrow indicates the η integration-path for $(\xi + \eta) < 0$

$$\frac{\xi - \beta + 2\gamma}{\xi + \eta + \beta + \gamma} < x. \quad (16)$$

We have two possibilities $\xi + \eta + \beta + \gamma > 0$ and $\xi + \eta + \beta + \gamma < 0$, in any case we have two limiting planes:

$$\xi(1-x) + \beta(-1-x) - \eta x + \gamma(2-x) = 0 \quad \text{and} \quad \xi + \eta + \beta + \gamma = 0$$

for $x < 0$ the traces of these two planes in the plane η, ξ are these of figure. 8.

Let us see the case with $\beta > 0$, $\gamma > 0$ and $\beta = b$ and $\gamma = g$. We have two conditions that define the allowed regions of the random variables, for this it will be possible to consider two of the four

variables completely unconstrained. The constraint will be applied to the variables ξ and η as done always. The variables ξ and η must be contained within the two planes of fig. 9. The intersection point is $\{-2b + g, b - 2g\}$ and now it follows the values of β and γ . Evidently, the only change in moving from $\beta > 0$ and $\gamma > 0$ to $\beta < 0$ and $\gamma < 0$ or any other combination of signs is a shift of the intersection point, and each line of the plot moves parallel to itself.

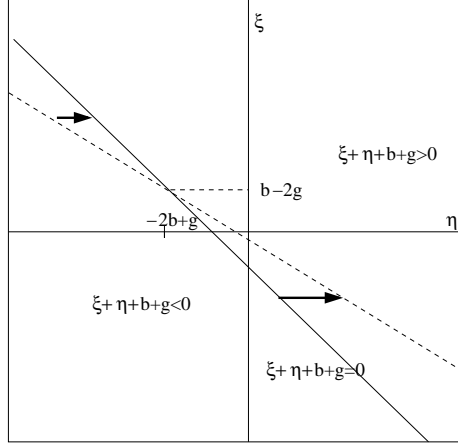


Figure 9: Sector of the plane (η, ξ) for a fixed value of $\beta = b$ and $\gamma = g$ where $\xi + \eta + b + g > 0$ or $\xi + \eta + b + g < 0$ and its boundary $\xi + \eta + b + g = 0$, the dashed line has the equation $\xi(1-x) + b(-1-x) - \eta x + g(2-x) = 0$ for negative x , the arrows indicate the η integration-paths for $(\xi + \eta + b + g) < 0$ and for $(\xi + \eta + b + g) > 0$. The intersection point of the two boundary lines is $\{-2b + g, b - 2g\}$

As for the three strip case $F_1^{xg^4}(x)$ becomes ($x < 0$):

$$F_1^{xg^4}(x) = \int_{-\infty}^{\infty} d\gamma P_4(\gamma) \int_{-\infty}^{\infty} d\beta P_3(\beta) \int_{\beta-2\gamma}^{\infty} d\xi P_1(\xi) \int_{\xi \frac{(1-x)}{x} + \beta \frac{(-1-x)}{x} + \gamma \frac{2-x}{x}}^{-\xi - \beta - \gamma} P_2(\eta) d\eta + \int_{-\infty}^{\infty} d\gamma P_4(\gamma) \int_{-\infty}^{\infty} d\beta P_3(\beta) \int_{-\infty}^{\beta-2\gamma} d\xi P_1(\xi) \int_{-\xi - \beta - \gamma}^{\xi \frac{(1-x)}{x} + \beta \frac{(-1-x)}{x} + \gamma \frac{2-x}{x}} P_2(\eta) d\eta \quad (17)$$

For $x \geq 0$ the traces of the two planes for $\beta = 0$ and $\gamma = 0$ are illustrated in fig. 10. With $\beta \neq 0$ and $\gamma \neq 0$, the traces of the two planes become these of fig. 11. The arrows indicate the integration paths. The intersection of the two lines are always in the point $\{-2b + g, b - 2g\}$ and the $F_2^{xg^4}(x)$ becomes:

$$F_2^{xg^4}(x) = \int_{-\infty}^{\infty} d\gamma P_4(\gamma) \int_{-\infty}^{\infty} d\beta P_3(\beta) \int_{-\infty}^{\beta-2\gamma} d\xi P_1(\xi) \int_{-\xi - \beta - \gamma}^{\infty} P_2(\eta) d\eta + \int_{-\infty}^{\infty} d\gamma P_4(\gamma) \int_{-\infty}^{\infty} d\beta P_3(\beta) \int_{\beta-2\gamma}^{\infty} d\xi P_1(\xi) \int_{\xi \frac{(1-x)}{x} + \beta \frac{(-1-x)}{x} + \gamma \frac{2-x}{x}}^{+\infty} P_2(\eta) d\eta + \int_{-\infty}^{\infty} d\gamma P_4(\gamma) \int_{-\infty}^{\infty} d\beta P_3(\beta) \int_{-\infty}^{\beta-2\gamma} d\xi P_1(\xi) \int_{-\infty}^{\xi \frac{(1-x)}{x} + \beta \frac{(-1-x)}{x} + \gamma \frac{2-x}{x}} P_2(\eta) d\eta + \int_{-\infty}^{\infty} d\gamma P_4(\gamma) \int_{-\infty}^{\infty} d\beta P_3(\beta) \int_{\beta-2\gamma}^{+\infty} d\xi P_1(\xi) \int_{-\infty}^{-\xi - \beta - \gamma} P_2(\eta) d\eta \quad (18)$$

As for x_{g3} , it is easy to prove that $\lim_{x \rightarrow -\infty} F_1^{xg^4}(x) = 0$ and $\lim_{x \rightarrow +\infty} F_2^{xg^4}(x) = 1$. In fact the first limit is easy given that $\lim_{x \rightarrow \pm\infty} (\pm 1 - x)/x = -1$ and $\lim_{x \rightarrow \pm\infty} (2 - x)/x = -1$. With this position eq. 17 has the limits of the last integrals identical, and the integrals are zero.

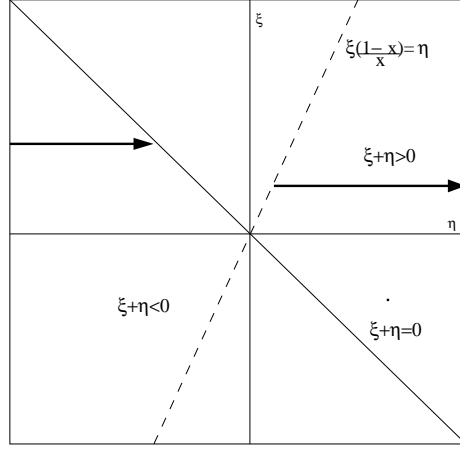


Figure 10: Sector of the plane (η, ξ) with $\beta = 0$ and $\gamma = 0$ where $\xi + \eta > 0$ or $\xi + \eta < 0$ and its boundary $\xi + \eta = 0$, the dashed line is the line $\xi(1-x)/x = \eta$ for positive x . The arrows indicate the integration regions and these must cover positive and negative values of ξ

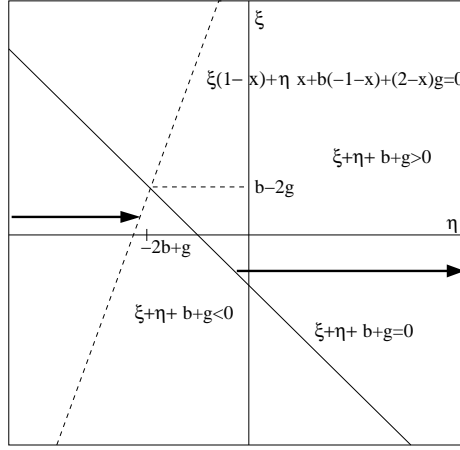


Figure 11: Sector of the plane (η, ξ) where $\xi + \eta + b + g > 0$ or $\xi + \eta + b + g < 0$ and its boundary $\xi + \eta + b + g = 0$, the dashed line is the line $\xi(1-x) - x\eta + b(-1-x) + g(2-x) = 0$ for $x > 0$. The arrows indicate the integration regions and these must cover positive and negative values of ξ

For $x \rightarrow +\infty$ the integrals of eq. 18 become:

$$\begin{aligned}
F_2^{xg^4}(+\infty) = & \int_{-\infty}^{\infty} d\gamma P_4(\gamma) \int_{-\infty}^{\infty} d\beta P_3(\beta) \int_{-\infty}^{\beta-2\gamma} d\xi P_1(\xi) \int_{-\xi-\beta-\gamma}^{\infty} P_2(\eta) d\eta + \\
& \int_{-\infty}^{\infty} d\gamma P_4(\gamma) \int_{-\infty}^{\infty} d\beta P_3(\beta) \int_{\beta-2\gamma}^{\infty} d\xi P_1(\xi) \int_{-\xi-\beta-\gamma}^{+\infty} P_2(\eta) d\eta + \\
& \int_{-\infty}^{\infty} d\gamma P_4(\gamma) \int_{-\infty}^{\infty} d\beta P_3(\beta) \int_{-\infty}^{\beta-2\gamma} d\xi P_1(\xi) \int_{-\infty}^{-\xi-\beta-\gamma} P_2(\eta) d\eta \\
& \int_{-\infty}^{\infty} d\gamma P_4(\gamma) \int_{-\infty}^{\infty} d\beta P_3(\beta) \int_{\beta-2\gamma}^{+\infty} d\xi P_1(\xi) \int_{-\infty}^{-\xi-\beta-\gamma} P_2(\eta) d\eta
\end{aligned} \tag{19}$$

The first and third integral have identical integration limits in the variables γ, β and ξ , and the sum of the last integrals produces the normalization of the probability distribution $P_2(\eta)$. Identically for the second

and forth integrals. The two remaining integrals add completing the normalization of the probability $P_1(\xi)$ that is multiplied by the normalization of $P_3(\beta)$ and $P_4(\gamma)$ giving 1.

Now, after this consistency check, we can extract the probability $P_{xg3}(x)$ differentiating $F_1^{xg4}(x)$ and $F_2^{xg4}(x)$ respect to x . The result is:

$$P_{xg4}(x) = \frac{1}{x^2} \left[\int_{-\infty}^{\infty} d\gamma P_4(\gamma) \int_{-\infty}^{+\infty} d\beta P_3(\beta) \int_{\beta-2\gamma}^{+\infty} d\xi P_1(\xi) P_2\left(\xi \frac{1-x}{x} + \beta \frac{-1-x}{x} + \gamma \frac{2-x}{x}\right) (-\beta + \xi + 2\gamma) + \int_{-\infty}^{\infty} d\gamma P_4(\gamma) \int_{-\infty}^{+\infty} d\beta P_3(\beta) \int_{-\infty}^{\beta-2\gamma} d\xi P_1(\xi) P_2\left(\xi \frac{1-x}{x} + \beta \frac{-1-x}{x} + \gamma \frac{2-x}{x}\right) (\beta - \xi - 2\gamma) \right] \quad (20)$$

With the transformation $\delta = \xi - \beta + 2\gamma$, eq. 20 becomes:

$$P_{xg4}(x) = \frac{1}{x^2} \left[\int_{-\infty}^{\infty} d\gamma P_4(\gamma) \int_{-\infty}^{+\infty} d\beta P_3(\beta) \int_0^{+\infty} d\delta P_1(\delta + \beta - 2\gamma) P_2\left(\delta \frac{1-x}{x} - 2\beta + \gamma\right) \delta - \int_{-\infty}^{\infty} d\gamma P_4(\gamma) \int_{-\infty}^{+\infty} d\beta P_3(\beta) \int_{-\infty}^0 d\delta P_1(\delta + \beta - 2\gamma) P_2\left(\delta \frac{1-x}{x} - 2\beta + \gamma\right) \delta \right] \quad (21)$$

or better:

$$P_{xg4}(x) = \frac{1}{x^2} \left[\int_{-\infty}^{\infty} d\gamma P_4(\gamma) \int_{-\infty}^{+\infty} d\beta P_3(\beta) \int_{-\infty}^{+\infty} d\delta P_1(\delta + \beta - 2\gamma) P_2\left(\delta \frac{1-x}{x} - 2\beta + \gamma\right) \text{abs}(\delta) \right] \quad (22)$$

This can be recast in a form more appropriate for its use with gaussian probability distributions:

$$P_{xg4}(x) = \frac{1}{x^2} \left[\int_{-\infty}^{+\infty} d\delta \text{abs}(\delta) \int_{-\infty}^{\infty} d\gamma P_4(\gamma) \int_{-\infty}^{+\infty} d\beta P_3(\beta) P_1(\delta + \beta - 2\gamma) P_2\left(\delta \frac{1-x}{x} - 2\beta + \gamma\right) \right] \quad (23)$$

Most of the approach for the right strip can be reused for the left strip, in this case the COG_4 algorithm is given:

$$x_5 = \psi, \quad x_3 = \beta, \quad x_2 = \eta, \quad x_1 = \xi, \quad x_4 = \gamma \quad x_{g4l} = \frac{\xi - \beta - 2\psi}{\xi + \eta + \beta + \psi} 1, .$$

Our condition is:

$$\frac{\xi - \beta - 2\psi}{\xi + \eta + \beta + \psi} < x. \quad (24)$$

This condition limits the random variables to be contained in regions bounded by the two planes:

$$\xi(1-x) + \beta(-1-x) - \eta x + \psi(-2-x) = 0 \quad \text{and} \quad \xi + \eta + \beta + \psi = 0.$$

The two planes intersect in the η, ξ -plane in the point $-2b - 3p, b + 2p$ if $\beta = b$ and $\psi = p$. In any case the developments are very similar to these performed for the right-strip case. The random variable ψ has probability distribution $P_5(\psi)$. Hence, $F_2^{xg4}(x)$ becomes ($x < 0$):

$$F_3^{xg4}(x) = \int_{-\infty}^{\infty} d\psi P_5(\psi) \int_{-\infty}^{\infty} d\beta P_3(\beta) \int_{\beta+2\psi}^{\infty} d\xi P_1(\xi) \int_{\xi \frac{(1-x)}{x} + \beta \frac{(-1-x)}{x} + \psi \frac{-2-x}{x}}^{-\xi - \beta - \psi} P_2(\eta) d\eta + \int_{-\infty}^{\infty} d\psi P_5(\psi) \int_{-\infty}^{\infty} d\beta P_3(\beta) \int_{-\infty}^{\beta+2\psi} d\xi P_1(\xi) \int_{-\xi - \beta - \psi}^{\xi \frac{(1-x)}{x} + \beta \frac{(-1-x)}{x} + \psi \frac{-2-x}{x}} P_2(\eta) d\eta \quad (25)$$

For $x \geq 0$ the probability $F_4^{xg4}(x)$ becomes:

$$\begin{aligned}
F_4^{xg4}(x) = & \int_{-\infty}^{\infty} d\psi P_5(\psi) \int_{-\infty}^{\infty} d\beta P_3(\beta) \int_{-\infty}^{\beta+2\psi} d\xi P_1(\xi) \int_{-\xi-\beta-\psi}^{\infty} P_2(\eta) d\eta + \\
& \int_{-\infty}^{\infty} d\psi P_5(\psi) \int_{-\infty}^{\infty} d\beta P_3(\beta) \int_{\beta+2\psi}^{\infty} d\xi P_1(\xi) \int_{\xi \frac{(1-x)}{x} + \beta \frac{(-1-x)}{x} + \psi \frac{-2-x}{x}}^{+\infty} P_2(\eta) d\eta + \\
& \int_{-\infty}^{\infty} d\psi P_5(\psi) \int_{-\infty}^{\infty} d\beta P_3(\beta) \int_{-\infty}^{\beta+2\psi} d\xi P_1(\xi) \int_{-\infty}^{\xi \frac{(1-x)}{x} + \beta \frac{(-1-x)}{x} + \psi \frac{-2-x}{x}} P_2(\eta) d\eta \\
& \int_{-\infty}^{\infty} d\psi P_5(\psi) \int_{-\infty}^{\infty} d\beta P_3(\beta) \int_{\beta+2\psi}^{+\infty} d\xi P_1(\xi) \int_{-\infty}^{-\xi-\beta-\psi} P_2(\eta) d\eta.
\end{aligned} \tag{26}$$

As above, it is easy to verify that $\lim_{x \rightarrow -\infty} F_3^{xg4}(x) = 0$ and $\lim_{x \rightarrow +\infty} F_4^{xg4}(x) = 1$. The derivative of eq. 26 respect to x gives the PDF of x :

$$\begin{aligned}
P_{xg4}^l(x) = & \frac{1}{x^2} \left[\int_{-\infty}^{\infty} d\psi P_5(\psi) \int_{-\infty}^{+\infty} d\beta P_3(\beta) \int_{\beta+2\psi}^{+\infty} d\xi P_1(\xi) P_2\left(\xi \frac{1-x}{x} + \beta \frac{-1-x}{x} + \psi \frac{-2-x}{x}\right) (-\beta + \xi - 2\psi) + \right. \\
& \left. \int_{-\infty}^{\infty} d\psi P_5(\psi) \int_{-\infty}^{+\infty} d\beta P_3(\beta) \int_{-\infty}^{\beta+2\psi} d\xi P_1(\xi) P_2\left(\xi \frac{1-x}{x} + \beta \frac{-1-x}{x} + \psi \frac{-2-x}{x}\right) (\beta - \xi + 2\psi) \right]
\end{aligned} \tag{27}$$

With the transformation $\delta = \xi - \beta - 2\psi$, eq. 27 becomes:

$$\begin{aligned}
P_{xg4}^l(x) = & \frac{1}{x^2} \left[\int_{-\infty}^{\infty} d\psi P_5(\psi) \int_{-\infty}^{+\infty} d\beta P_3(\beta) \int_0^{+\infty} d\delta P_1(\delta + \beta + 2\psi) P_2\left(\delta \frac{1-x}{x} - 2\beta - 3\psi\right) \delta - \right. \\
& \left. \int_{-\infty}^{\infty} d\psi P_5(\psi) \int_{-\infty}^{+\infty} d\beta P_3(\beta) \int_{-\infty}^0 d\delta P_1(\delta + \beta + 2\psi) P_2\left(\delta \frac{1-x}{x} - 2\beta - 3\psi\right) \delta \right]
\end{aligned} \tag{28}$$

or better:

$$P_{xg4}^l(x) = \frac{1}{x^2} \left[\int_{-\infty}^{\infty} d\psi P_5(\psi) \int_{-\infty}^{+\infty} d\beta P_3(\beta) \int_{-\infty}^{+\infty} d\delta P_1(\delta + \beta + 2\psi) P_2\left(\delta \frac{1-x}{x} - 2\beta - 3\psi\right) \text{abs}(\delta) \right] \tag{29}$$

This can be recast in a form more appropriate for the use with Gaussian PDFs of the signals:

$$P_{xg4}^l(x) = \frac{1}{x^2} \left[\int_{-\infty}^{+\infty} d\delta \text{abs}(\delta) \int_{-\infty}^{\infty} d\psi P_5(\psi) \int_{-\infty}^{+\infty} d\beta P_3(\beta) P_1(\delta + \beta + 2\psi) P_2\left(\delta \frac{1-x}{x} - 2\beta - 3\psi\right) \right] \tag{30}$$

3.2 Complete probability distribution for $P_{xg4}(x)$

The two probability density functions, calculated up to now, are only a part of the full probability distribution for the COG₄ algorithm. In fact, the COG₄ algorithm is composed by the three internal strips and the strip with maximum signal selected from the two lateral strips ($< 5 >$ and $< 4 >$). We have to add this further condition. When the left strip has a signal greater than the right one $P_{xg4}(x)$ converges toward $P_{xg4}^l(x)$. If the greater strip signal is the right one, $P_{xg4}(x)$ converges toward $P_{xg4}^r(x)$.

$$\begin{aligned}
P_{xg4}(x) = & \frac{1}{x^2} \left[\int_{-\infty}^{\infty} d\psi P_5(\psi) \int_{\psi}^{\infty} d\gamma P_4(\gamma) \int_{-\infty}^{+\infty} d\beta P_3(\beta) \int_{-\infty}^{+\infty} d\delta P_1(\delta + \beta - 2\gamma) P_2\left(\delta \frac{1-x}{x} - 2\beta + \gamma\right) \text{abs}(\delta) + \right. \\
& \left. \int_{-\infty}^{\infty} d\gamma P_4(\gamma) \int_{\gamma}^{\infty} d\psi P_5(\psi) \int_{-\infty}^{+\infty} d\beta P_3(\beta) \int_{-\infty}^{+\infty} d\delta P_1(\delta + \beta + 2\psi) P_2\left(\delta \frac{1-x}{x} - 2\beta - 3\psi\right) \text{abs}(\delta) \right]
\end{aligned} \tag{31}$$

Another form is given by the Fubini's theorem applied to the first two integrals:

$$P_{xg4}(x) = \frac{1}{x^2} \left[\int_{-\infty}^{\infty} d\gamma P_4(\gamma) \int_{-\infty}^{\gamma} d\psi P_5(\psi) \int_{-\infty}^{+\infty} d\beta P_3(\beta) \int_{-\infty}^{+\infty} d\delta P_1(\delta + \beta - 2\gamma) P_2\left(\delta \frac{1-x}{x} - 2\beta + \gamma\right) \text{abs}(\delta) + \right. \quad (32)$$

$$\left. \int_{-\infty}^{\infty} d\psi P_5(\psi) \int_{-\infty}^{\psi} d\gamma P_4(\gamma) \int_{-\infty}^{+\infty} d\beta P_3(\beta) \int_{-\infty}^{+\infty} d\delta P_1(\delta + \beta + 2\psi) P_2\left(\delta \frac{1-x}{x} - 2\beta - 3\psi\right) \text{abs}(\delta) \right]$$

With simple transformations (as $z = \delta/x$), the PDFs of ref. [4] are easily recovered. This last PDF and that with five strips of ref. [4] were principally conceived for the extraction of the detector parameters from the corresponding COG histograms with a self-consistent process. The explicit PDFs for Gaussian additive noise require extensive use of MATHEMATICA [15] and are reported in ref. [4].

4 Summary and conclusions

The probability density functions for center of gravity algorithms with three strips and four strips are computed with the classical method of differentiation of the corresponding cumulative distributions. These derivations, through the cumulative distributions, are consistent verifications of our published shorter methods. The probability density function for the three strip algorithm was extensively used in previous works for reproducing the corresponding histograms of the center of gravity and testing the detector parameters extracted from the data. In fact, the simulations performed at orthogonal incidence do not require these more complex probabilities, the two strips formalism suffices. Almost always, the third and fourth strips have no signal information, but essentially noise. Instead, the four and five strip algorithms can be used to a finer tuning of the detector parameters extracted from the data, the data histograms depend significantly on their values. These non-linear dependencies allow the construction of a self-consistent process for removing small artifacts of the first order reconstructions.

References

- [1] Landi G.; Landi G. E. *The Cramer-Rao inequality to improve of the resolution of the least-squares method in track fitting* INSTRUMENTS **2020**, 4(1), 2. <https://doi.org/10.3390/instruments4010002>
- [2] Landi G.; Landi G. E. *Generalized inequalities to optimizing the fitting method for track reconstructions*, Physics **2020** 2(4) <https://doi.org/10.3390/physics2040035>
- [3] Landi G.; Landi G. E.; *Probability Distributions of Positioning Errors for Some Forms of Center-of-Gravity Algorithms*. arXiv:2004.08975 [physics.ins-det]
- [4] Landi G.; Landi G. E.; *Probability Distributions of Positioning Errors for Some Forms of Center-of-Gravity Algorithms. Part II* arXiv:2011.14474 [physics.ins-det]
- [5] Landi, G.; Landi G. E. *Optimizing momentum resolution with a new fitting method for silicon-strip detectors* INSTRUMENTS **2018**, 2(4), 22 <https://doi.org/10.3390/instruments2040022>
- [6] B. V. Gnedenko "The Theory of Probability and Elements of Statistics" (AMS Chelsea Publishing -Providence Rhode Island)
- [7] Landi G.; Landi G. E.; *Positioning Error Probability for Some Forms of Center-of-Gravity Algorithms Calculated with the Cumulative Distributions. Part I*. arXiv:2006.02934[physics.ins-det]

- [8] Landi G.; Landi G. E. *Improvement of track reconstruction with well tuned robustness distributions* *JINST* 9 2014 P10006. arXiv:1404.1968[physics.ins-det] <https://arxiv.org/abs/1404.1968>
- [9] Landi G.; Landi G. E. *Beyond the \sqrt{N} -limit of the least squares resolution and the lucky-model* arXiv:1808.06708[physics.ins-det] <https://arxiv.org/abs/1808.06708>.
- [10] MatLab 8 The MathWork Inc. Natic, MA, USA
- [11] Frühwirth R.; *Regression with Gaussian mixture models applied to track fitting* *INSTRUMENTS* **2020**, 4(3) 25.
- [12] Bernard D. "Heteroscedasticity and angle resolution in high-energy particle tracking: revisiting "Beyond the \sqrt{N} limits of the least squares resolution and the lucky model", by G. Landi and G. E. Landi" arXiv:2010.03451[physics.ins-det]
- [13] G. Landi, *The center of gravity as an algorithm for position measurements* *Nucl. Instr. and Meth. A* **485** (2002) 698 arXiv:1908.04447 [physics.ins-det] <https://arxiv.org/abs/1910.04447>.
- [14] G. Landi, *Problems of position reconstruction in silicon microstrip detectors* *Nucl. Instr. and Meth. A* **554** (2005) 226.
- [15] MATHEMATICA 6 Wolfram Inc. Champaign IL, USA